



Short Communication

Etherification of n-butanol to di-n-butyl ether over $H_nXW_{12}O_{40}$ ($X=Co^{2+}$, B^{3+} , Si^{4+} , and P^{5+}) Keggin heteropolyacid catalysts

Jeong Kwon Kim, Jung Ho Choi, Ji Hwan Song, Jongheop Yi, In Kyu Song*

School of Chemical and Biological Engineering, Institute of Chemical Processes, Seoul National University, Shinlim-dong, Kwanak-ku, Seoul 151–744, South Korea

ARTICLE INFO

Article history:

Received 18 April 2012

Received in revised form 10 June 2012

Accepted 11 June 2012

Available online 18 June 2012

Keywords:

Etherification
Di-n-butyl ether
Heteropolyacid
Heteroatom
Acid strength

ABSTRACT

Etherification of n-butanol to di-n-butyl ether was carried out over heteroatom-substituted $H_nXW_{12}O_{40}$ ($X=Co^{2+}$, B^{3+} , Si^{4+} , and P^{5+}) Keggin heteropolyacid (HPA) catalysts. Acid properties of HPA catalysts were determined by NH_3 -TPD measurements. Acid strength of $H_nXW_{12}O_{40}$ Keggin HPA catalysts increased in the order of $H_6CoW_{12}O_{40} < H_5BW_{12}O_{40} < H_4SiW_{12}O_{40} < H_3PW_{12}O_{40}$. Yield for di-n-butyl ether increased with increasing acid strength of the catalysts. Acid strength of HPAs served as an important factor determining the catalytic performance in the etherification of n-butanol to di-n-butyl ether.

© 2012 Elsevier B.V. All rights reserved.

1. Introduction

Due to the current oil shortage, many researchers have made an effort to enhance the quality of diesel fuel. It has been reported that linear ethers (total number of atoms ≥ 9) can enhance the octane and cetane number of diesel fuel [1,2]. Linear ethers are also known to be effective additives to reduce diesel exhausts such as CO, NO_x , and unburned hydrocarbons [2,3]. Di-n-butyl ether has attracted recent attention, because it can be directly synthesized from bio-butanol obtained via pyrolysis of biomass. Linear ether is generally produced by bi-molecular dehydration of linear alcohol over acid catalysts. Conventional mineral acids and solid acid catalysts have been studied as a catalyst for the production of linear ether [4–7]. Solid acid catalysts such as zeolite, clay, and alumina generally exhibit a poor catalytic activity for linear ether production [5–7]. Although mineral acids such as sulfuric acid show a high catalytic activity for linear ether formation [4], much amount of alkyl sulfates is formed and corrosion of reaction system occurs. For effective linear ether production, therefore, it is necessary to find an environmentally benign catalyst that can give high activity and selectivity.

Heteropolyacids (HPAs) are early transition metal-oxygen anion cluster that exhibit a wide range of molecular sizes, composition, and architectures [8]. HPAs have attracted considerable attention as a promising acid catalyst in several homogeneous and heterogeneous reactions including hydration of propylene [9], Friedel–Craft reaction [10], MTBE synthesis [11], and ETBE synthesis [12]. HPA catalysts show stronger acid strength than several conventional mineral acids.

In addition, acid properties of HPAs can be easily controlled by changing constituent components such as charge-compensating counter-cation, heteroatom, and framework polyatom [13,14].

In this work, heteroatom-substituted $H_nXW_{12}O_{40}$ ($X=Co^{2+}$, B^{3+} , Si^{4+} , and P^{5+}) Keggin HPA catalysts were prepared for use in the etherification of n-butanol to di-n-butyl ether. Acid properties of HPA catalysts were determined by NH_3 -TPD measurements. The measured acid properties of HPA catalysts were then correlated with the catalytic performance in the etherification reaction.

2. Experimental

2.1. Preparation of HPA catalysts

Commercially available $H_3PW_{12}O_{40}$ and $H_4SiW_{12}O_{40}$ were obtained from Sigma-Aldrich. $K_5BW_{12}O_{40}$ and $K_6CoW_{12}O_{40}$ were prepared according to the methods in the literatures [15,16] using $Na_2WO_4 \cdot 2H_2O$ (Junsei Chem.), H_3BO_3 (Samchun Chem.), $Co(CH_3CO_2)_2 \cdot 4H_2O$ (Sigma-Aldrich), KCl (Junsei Chem.), hydrochloric acid (Sigma-Aldrich), acetic acid (Junsei Chem.), sulfuric acid (Samchun Chem.), and diethyl ether (Samchun Chem.). In order to convert as-prepared potassium salt into acid form, $K_5BW_{12}O_{40}$ and $K_6CoW_{12}O_{40}$ were treated with sulfuric acid and then extracted with diethyl ether (etherate method). $H_5BW_{12}O_{40}$ and $H_6CoW_{12}O_{40}$ were finally obtained after drying and recrystallization.

2.2. Characterization

Formation of $H_nXW_{12}O_{40}$ ($X=Co^{2+}$, B^{3+} , Si^{4+} , and P^{5+}) Keggin HPA catalysts was confirmed by FT-IR (Nicolet, Nicolet 6700) measurements. Chemical compositions of constituent elements in the $H_nXW_{12}O_{40}$

* Corresponding author. Tel.: +82 2 880 9227; fax: +82 2 889 7415.

E-mail address: inksong@snu.ac.kr (I.K. Song).

Keggin HPA catalysts were determined by ICP-AES (Shimadzu, ICP-1000IV) analyses. All the HPA catalysts were thermally treated at 200 °C in a stream of nitrogen prior to characterization and catalytic reaction.

Acid properties of $H_nXW_{12}O_{40}$ ($X=Co^{2+}$, B^{3+} , Si^{4+} , and P^{5+}) Keggin HPA catalysts were determined by NH_3 -TPD measurements. Each HPA catalyst (90 mg) was charged into a tubular quartz reactor of the TPD apparatus (BEL Japan, BELCAT B). Each catalyst was pretreated at 200 °C for 2 h under a flow of He (50 ml/min) to remove any physisorbed organic molecules. NH_3 (50 ml/min) was then introduced into the reactor at 50 °C for 30 min. Physisorbed NH_3 was removed at 100 °C for 1 h under a flow of He (50 ml/min). After cooling down the sample, furnace temperature was increased from room temperature to 700 °C at heating rate 5 °C/min under a flow of He (30 ml/min). The desorbed NH_3 was detected using a TCD (thermal conductivity detector).

2.3. Catalytic reaction

Etherification of n-butanol to di-n-butyl ether was carried out over $H_nXW_{12}O_{40}$ ($X=Co^{2+}$, B^{3+} , Si^{4+} , and P^{5+}) Keggin HPA catalysts in a stainless steel autoclave reactor (200 ml). 1 g of each HPA catalyst and a mixture of n-butanol (80 ml) and toluene (20 ml, reaction medium) were charged into the reactor at room temperature. The reactor was purged with nitrogen several times in order to remove air. The reactor was then heated to 200 °C. The reaction was carried out for 3 h at nitrogen pressure of 30 bar. After the reaction, reaction products were sampled and analyzed using a gas chromatograph (Younglin Corp., YL6100 GC-FID) equipped with a capillary column (Agilent, DB-5MS, 60 m × 0.320 mm). Conversion of n-butanol and selectivity for di-n-butyl ether were calculated according to the following equations [17]. Yield for di-n-butyl ether was calculated by multiplying conversion of n-butanol and selectivity for di-n-butyl ether.

$$\text{Conversion of n-butanol (\%)} = \frac{\text{mole of n-butanol reacted}}{\text{mole of n-butanol in the feed}} \times 100 \quad (1)$$

$$\text{Selectivity for di-n-butyl ether (\%)} = \frac{2 \times \text{mole of di-n-butyl ether formed}}{\text{mole of n-butanol reacted}} \times 100 \quad (2)$$

3. Results and discussion

3.1. Formation of $H_nXW_{12}O_{40}$ ($X=Co^{2+}$, B^{3+} , Si^{4+} , and P^{5+}) Keggin HPA catalysts

Successful formation of $H_nXW_{12}O_{40}$ ($X=Co^{2+}$, B^{3+} , Si^{4+} , and P^{5+}) Keggin HPA catalysts was confirmed by FT-IR analyses. Fig. 1 shows the FT-IR spectra of $H_nXW_{12}O_{40}$ ($X=Co^{2+}$, B^{3+} , Si^{4+} , and P^{5+}) Keggin HPA catalysts. Characteristic IR bands of Keggin heteropolyanions were clearly observed. IR band positions of heteropolyanions were in good agreement with the results in the previous works [15,18], indicating successful formation of heteropolyanion framework. Different X–O bonding nature and subsequent effect on the stretching vibrations of tungsten–oxygen bonds may bring about changes in IR bands of four heteropolyanions [19]. Successful formation of HPA catalysts was further confirmed by ICP-AES analyses. Chemical compositions of heteroatom and tungsten in the $H_nXW_{12}O_{40}$ ($X=Co^{2+}$, B^{3+} , Si^{4+} , and P^{5+}) HPA catalysts determined by ICP-AES analyses are summarized in Table 1. The measured X:W ratios in the $H_nXW_{12}O_{40}$ ($X=Co^{2+}$, B^{3+} , Si^{4+} , and P^{5+}) HPA catalysts were in good agreement with the theoretical values.

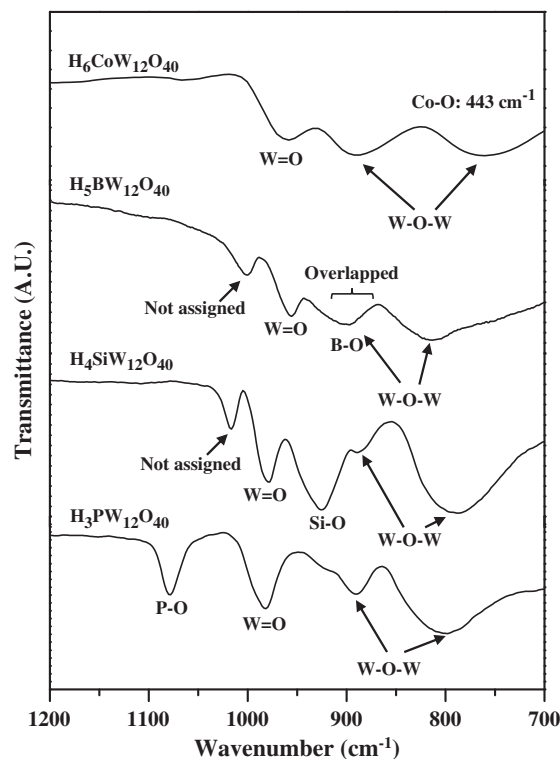


Fig. 1. FT-IR spectra of $H_nXW_{12}O_{40}$ ($X=Co^{2+}$, B^{3+} , Si^{4+} , and P^{5+}) Keggin HPA catalysts.

3.2. Acid properties of $H_nXW_{12}O_{40}$ ($X=Co^{2+}$, B^{3+} , Si^{4+} , and P^{5+}) Keggin HPA catalysts

NH_3 -TPD measurements were carried out to investigate acid properties of $H_nXW_{12}O_{40}$ ($X=Co^{2+}$, B^{3+} , Si^{4+} , and P^{5+}) Keggin HPA catalysts. Fig. 2 shows the NH_3 -TPD profiles of $H_nXW_{12}O_{40}$ ($X=Co^{2+}$, B^{3+} , Si^{4+} , and P^{5+}) Keggin HPA catalysts. It is noteworthy that three distinct desorption peaks were observed in the HPA catalysts. A desorption peak appearing in the range of 100–200 °C (denoted as α -peak) was due to the desorption of hydrogen-bonded NH_3 molecules [20]. A desorption peak appearing in the range of 200–465 °C (denoted as β -peak) was due to the decomposition of ionically bonded NH_4^+ ions that contact with oxygen atom of one Keggin unit [20]. A desorption peak appearing in the range of 465–600 °C (denoted as γ -peak) was due to the decomposition of ionically bonded NH_4^+ ions that contact with oxygen atom between two neighboring Keggin units [20]. Because bond strength of ionically bonded NH_4^+ ions is stronger than that of hydrogen-bonded NH_3 molecules, β -peak and γ -peak appeared at higher temperatures than α -peak. Difference in desorption peak temperature between β -peak and γ -peak was due to the decomposition of NH_4^+ ions with different location and coordination in the crystal lattice.

Desorption peak temperatures of $H_nXW_{12}O_{40}$ ($X=Co^{2+}$, B^{3+} , Si^{4+} , and P^{5+}) Keggin HPA catalysts are summarized in Table 2. α -peak and β -peak were much weaker than γ -peak, and only γ -peak exhibited a consistent result with acid strength measured by Hammett indicator

Table 1

Chemical compositions of heteroatom and tungsten in the $H_nXW_{12}O_{40}$ ($X=Co^{2+}$, B^{3+} , Si^{4+} , and P^{5+}) HPA catalysts determined by ICP-AES analyses.

| Catalyst | Ratio of X:W ($X=P, Si, B, Co$) | |
|---------------------|-----------------------------------|----------------|
| | Theoretical value | Measured value |
| $H_3PW_{12}O_{40}$ | 1.0:12.0 | 1.1:12.0 |
| $H_4SiW_{12}O_{40}$ | 1.0:12.0 | 1.0:12.0 |
| $H_5BW_{12}O_{40}$ | 1.0:12.0 | 1.1:12.0 |
| $H_6CoW_{12}O_{40}$ | 1.0:12.0 | 1.1:12.0 |

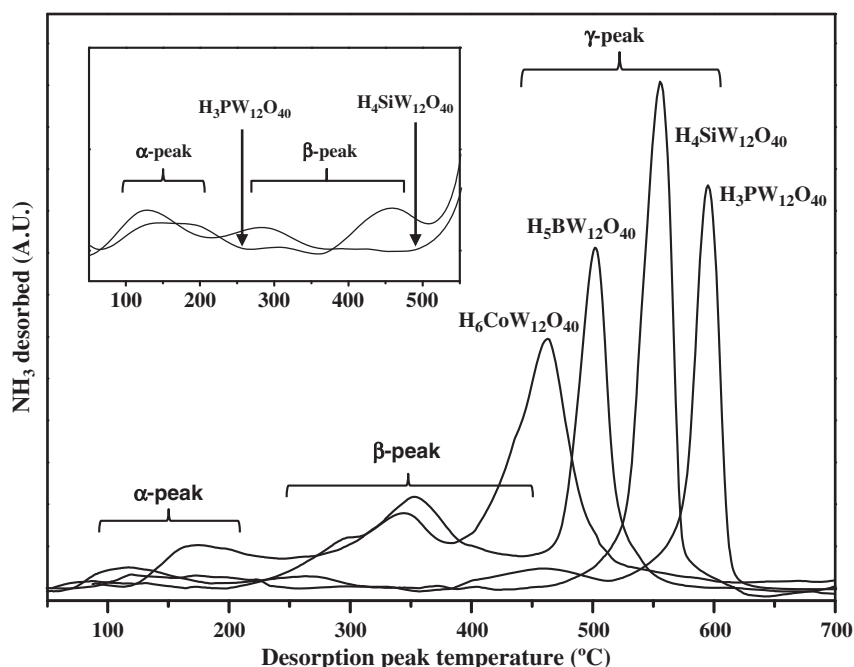


Fig. 2. NH_3 -TPD profiles of $\text{H}_n\text{XW}_{12}\text{O}_{40}$ ($\text{X}=\text{Co}^{2+}$, B^{3+} , Si^{4+} , and P^{5+}) Keggin HPA catalysts.

[14]. In this work, therefore, peak temperature of γ -peak was taken as an index for acid strength of the catalysts. Acid strength increased in the order of $\text{H}_6\text{CoW}_{12}\text{O}_{40}$ (469 °C) < $\text{H}_5\text{BW}_{12}\text{O}_{40}$ (501 °C) < $\text{H}_4\text{SiW}_{12}\text{O}_{40}$ (568 °C) < $\text{H}_3\text{PW}_{12}\text{O}_{40}$ (593 °C). Among the catalysts examined, $\text{H}_3\text{PW}_{12}\text{O}_{40}$ catalyst exhibited the strongest acid strength.

It has been reported that electrostatic attractive interaction (Coulombic force) between proton and heteropolyanion is proportional to the product of amount of individual charges [14]. In case of heteroatom-substituted $\text{H}_n\text{XW}_{12}\text{O}_{40}$ Keggin HPA catalysts, valence of heteroatom determines the overall charge of heteropolyanion. Overall charge of the heteropolyanion became less negative with increasing valence of heteroatom. Because variation of molecular size of Keggin heteropolyanion is negligible, less negative overall charge of heteropolyanion may give weaker interaction between proton and heteropolyanion. Weaker interaction between proton and heteropolyanion enables proton to be easily released, resulting in stronger acid strength [14]. Fig. 3 shows the correlation between desorption peak temperature of γ -peak and overall charge of heteropolyanion. As expected, desorption peak temperature (acid strength) of $\text{H}_n\text{XW}_{12}\text{O}_{40}$ Keggin HPA catalysts increased with decreasing overall negative charge of heteropolyanion (with increasing valence of heteroatom). Thus, acid strength of HPA catalysts could be easily controlled by changing heteroatom.

3.3. Etherification of *n*-butanol to di-*n*-butyl ether over $\text{H}_n\text{XW}_{12}\text{O}_{40}$ ($\text{X}=\text{Co}^{2+}$, B^{3+} , Si^{4+} , and P^{5+}) Keggin HPA catalysts

According to the literature [21], dehydration of linear alcohols follows parallel-consecutive reaction pathway. In the catalytic dehydration

of *n*-butanol over Brönsted acid site, di-*n*-butyl ether is produced via intermolecular dehydration of *n*-butanol. On the other hand, 1-butene, which can be isomerized into *cis*-2-butene and *trans*-2-butene, is produced via intramolecular dehydration. Olefin formation is thermodynamically favorable with increasing reaction temperature [22]. At reaction temperature higher than 200 °C, selectivity for di-*n*-butyl ether remarkably decreases with increasing temperature [17]. In this work, therefore, catalytic reaction was conducted at 200 °C and 30 bar for efficient production of di-*n*-butyl ether.

Fig. 4 shows the catalytic performance of $\text{H}_n\text{XW}_{12}\text{O}_{40}$ ($\text{X}=\text{Co}^{2+}$, B^{3+} , Si^{4+} , and P^{5+}) Keggin HPA catalysts in the etherification of *n*-butanol to di-*n*-butyl ether at 200 °C after a 3 h-reaction. Selectivity for di-*n*-butyl ether over all HPA catalysts was higher than 90%, while selectivity for butenes (including 1-butene, *cis*-2-butene, and *trans*-2-butene) was less than 5%. Any oxidation products were not detected. Yield for di-*n*-butyl ether increased in the order of $\text{H}_6\text{CoW}_{12}\text{O}_{40}$ (26.5%) < $\text{H}_5\text{BW}_{12}\text{O}_{40}$ (52.1%) < $\text{H}_4\text{SiW}_{12}\text{O}_{40}$ (62.5%) < $\text{H}_3\text{PW}_{12}\text{O}_{40}$ (73.2%). Such a high catalytic activity might be derived from unique properties of HPA catalysts such as softness, strong acid strength, and excellent acidity [14]. Reaction

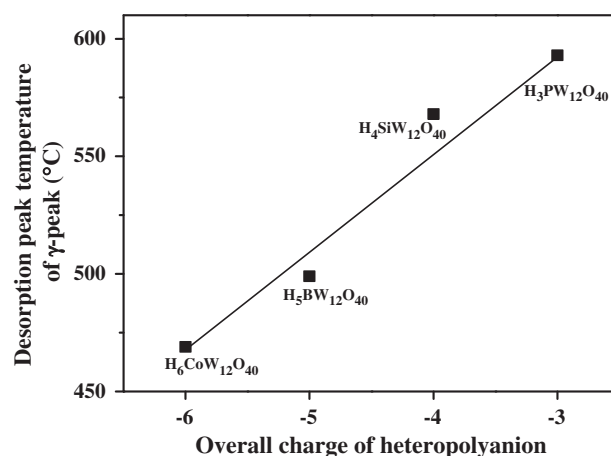


Fig. 3. A correlation between desorption peak temperature of γ -peak and overall charge of heteropolyanion.

Table 2

Desorption peak temperatures of $\text{H}_n\text{XW}_{12}\text{O}_{40}$ ($\text{X}=\text{Co}^{2+}$, B^{3+} , Si^{4+} , and P^{5+}) Keggin HPA catalysts.

| Catalyst | Desorption peak temperature (°C) | | |
|--|----------------------------------|---------------|----------------|
| | α -peak | β -peak | γ -peak |
| $\text{H}_3\text{PW}_{12}\text{O}_{40}$ | 152 | 463 | 593 |
| $\text{H}_4\text{SiW}_{12}\text{O}_{40}$ | 132 | 297 | 568 |
| $\text{H}_5\text{BW}_{12}\text{O}_{40}$ | 128 | 349 | 501 |
| $\text{H}_6\text{CoW}_{12}\text{O}_{40}$ | 112 | 346 | 496 |

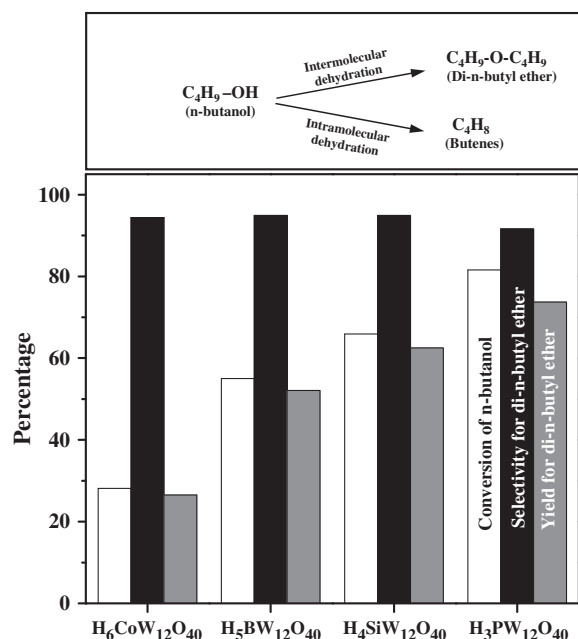


Fig. 4. Catalytic performance of $H_nXW_{12}O_{40}$ ($X=Co^{2+}$, B^{3+} , Si^{4+} , and P^{5+}) Keggin HPA catalysts in the etherification of n-butanol to di-n-butyl ether at 200 °C after a 3 h-reaction.

intermediates including oxonium or carbenium ions can be selectively coordinated and stabilized on the surface of heteropolyanion via formation of intermediate-heteropolyanion complex due to the softness of heteropolyanion [14]. It is known that softness of $SiW_{12}O_{40}^{4-}$ is greater than that of $PW_{12}O_{40}^{3-}$ [14]. In some particular aqueous reactions, softness becomes a dominant factor due to complete dissociation of heteropolyacid into heteropolyanion. In this case, the catalytic performance of $H_4SiW_{12}O_{40}$ catalyst would be better than that of $H_3PW_{12}O_{40}$ catalyst. In the etherification of n-butanol to di-n-butyl ether, however, the catalytic performance of HPA catalysts was not proportional to the softness of heteropolyanions. Therefore, our next investigation was focused on the acid properties of HPA catalysts. However, no correlation between acidity and catalytic performance was found. Instead, experimental results revealed that the trend of yield for di-n-butyl ether was well consistent with the trend of acid strength (desorption peak temperature of γ -peak). Therefore, it is concluded that acid strength of HPA catalysts dominantly affected the catalytic performance in the etherification of n-butanol.

Fig. 5 shows the correlations of desorption peak temperature of γ -peak with conversion of n-butanol and with yield for di-n-butyl ether at 200 °C after a 3 h-reaction. Conversion of n-butanol and yield for di-n-butyl ether increased with increasing desorption peak temperature of γ -peak (with increasing acid strength) of HPA catalysts. This result indicates that acid strength played a key role in the etherification of n-butanol over $H_nXW_{12}O_{40}$ Keggin HPA catalysts.

4. Conclusion

Etherification of n-butanol to di-n-butyl ether was carried out over heteroatom-substituted $H_nXW_{12}O_{40}$ ($X=Co^{2+}$, B^{3+} , Si^{4+} , and P^{5+}) Keggin HPA catalysts in a liquid-phase batch reactor. $H_nXW_{12}O_{40}$ Keggin HPA catalysts were prepared and characterized by FT-IR and ICP-AES analyses. Acid properties of $H_nXW_{12}O_{40}$ Keggin HPA catalysts were

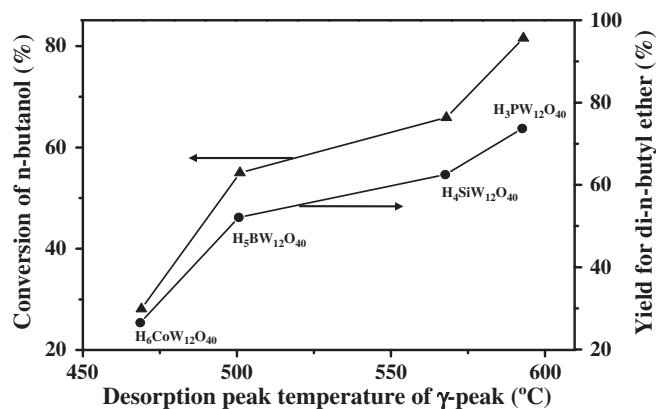


Fig. 5. Correlations of desorption peak temperature of γ -peak with conversion of n-butanol and with yield for di-n-butyl ether at 200 °C after a 3 h-reaction.

determined by NH_3 -TPD measurements. Desorption peak temperature of γ -peak (acid strength) increased in the order $H_6CoW_{12}O_{40}$ (469 °C) < $H_5BW_{12}O_{40}$ (501 °C) < $H_4SiW_{12}O_{40}$ (568 °C) < $H_3PW_{12}O_{40}$ (593 °C). In the etherification of n-butanol to di-n-butyl ether over $H_nXW_{12}O_{40}$ Keggin HPA catalysts, yield for di-n-butyl ether increased with increasing acid strength of the catalysts. It is concluded that acid strength of HPA catalysts, which was easily controlled by changing heteroatom, played an important role in the etherification of n-butanol to di-n-butyl ether over $H_nXW_{12}O_{40}$ ($X=Co^{2+}$, B^{3+} , Si^{4+} , and P^{5+}) Keggin HPA catalysts.

Acknowledgments

This subject is supported by Korea Ministry of Environment as “Converging Technology Project (202-101-009)”.

References

- [1] J. Tejero, F. Cunill, M. Iborra, J.F. Izquierdo, C. Fitè, *Journal of Molecular Catalysis A: Chemical* 182 (2002) 541.
- [2] J.J. Reinier, A.D. Klerk, *Industrial and Engineering Chemistry Research* 48 (2009) 5230.
- [3] A. Golubkov, WO Patent 01/018154 (2001).
- [4] K.R. Sabu, R. Sukumar, R. Rekha, M. Lalithambika, *Catalysis Today* 49 (1999) 321.
- [5] M.A. Makarova, E.A. Paukshtis, J.M. Thomas, C. Williams, K.I. Azamaraev, *Journal of Catalysis* 149 (1994) 36.
- [6] V. Bokade, G.D. Yadav, *Applied Clay Science* 53 (2011) 263.
- [7] N.P. Makgoba, T.M. Sakuneka, J.G. Koortzen, C. Schalkwyk, J.M. Botha, C.P. Nicolaidis, *Applied Catalysis A* 297 (2006) 145.
- [8] M. Misono, *Catalysis Reviews—Science and Engineering* 29 (1987) 269.
- [9] Y. Onoue, Y. Mizutani, S. Akiyama, Y. Izumi, *ChemTech* (1978) 432.
- [10] Y. Izumi, M. Ogawa, K. Urabe, *Applied Catalysis* 132 (1995) 846.
- [11] S. Shikata, S.I. Nakata, T. Okuhara, M. Misono, *Journal of Catalysis* 166 (1997) 263.
- [12] A. Bielański, A. Lubańska, A. Micek-Ilńska, J. Poźniczek, *Coordination Chemistry Reviews* 249 (2005) 2222.
- [13] I.V. Kozhevnikov, *Chemical Reviews* 98 (1998) 171.
- [14] T. Okuhara, N. Mizuno, M. Misono, *Advances in Catalysis* 41 (1996) 113.
- [15] C. Rocchiccioli-Deltcheff, M. Fournier, R. Frank, *Inorganic Chemistry* 22 (1983) 207.
- [16] L.C.W. Baker, T.P. Mccutcheon, *Journal of the American Chemical Society* 78 (1956) 4503.
- [17] J.H. Choi, J.K. Kim, D.R. Park, S. Park, J. Yi, I.K. Song, *Catalysis Communications* 14 (2011) 48.
- [18] C. Rocchiccioli-Deltcheff, R. Thouvenot, R. Frank, *Spectrochimica Acta Part A* 32 (1976) 437.
- [19] M.T. Pope, *Heteropoly and Isopoly Oxometalates*, Springer-Verlag, New York, 1983.
- [20] A. Bielański, A. Cichowlas, D. Kostrzewa, A. Malecka, *Zeitschrift für Physikalische Chemie* 167 (1990) 93.
- [21] S. Yoshinori, N.C. Park, N. Hirro, E. Etsuro, *Journal of Catalysis* 95 (1985) 49.
- [22] H. Knözinger, R. Köhn, *Journal of Catalysis* 5 (1966) 264.